ELSEVIER

Biochimica et Biophysica Acta 1196 (1994) 172–180

BBA Biochimica et Biophysica Acta

Influence of dye and protein location on photosensitization of the plasma membrane

Irene E. Kochevar [a,*], Joseph Bouvier [a], Mary Lynch [a], Chi-Wei Lin [b]

[a] *Wellman Laboratories of Photomedicine, Department of Dermatology, Massachusetts General Hospital, WEL-224, Boston, MA 02114, USA*
[b] *Department of Urology, Massachusetts General Hospital, Harvard Medical School, Boston, MA, USA*

Received 11 April 1994; revised 12 September 1994

Abstract

Two membrane-photosensitizing dyes were used to investigate whether selected sites in the plasma membrane vary in their sensitivity to damage by singlet oxygen ($^1O_2^*$) and, if so, what factors are responsible for the variation. The relative ability of Rose bengal (RB) and merocyanine 540 (MC540), both of which localize in the plasma membrane and produce $^1O_2^*$, to photosensitize five plasma membrane functions in P388D$_1$ cells was evaluated. The five membrane functions assessed were: plasma membrane potential, proline transport, facilitated glucose diffusion, 5′-nucleotidase activity, and dye exclusion. Photosensitization efficiency by RB varied by a factor of 188 for these membrane functions, whereas for MC540 a range of only 24 was found. RB was a more efficient photosensitizer than MC540 but the relative efficiencies varied with the membrane function. The wide range of P_{50} values for RB suggests that it binds selectively to membrane sites where it causes damage with high efficiency; possibly a non-$^1O_2^*$ mechanism is involved. In contrast, MC540 photosensitized the three membrane functions involving integral membrane proteins about equally suggesting that differences are due to small variations in the distribution of MC540 in the plasma membrane and/or variations in the inherent reactivity of the membrane targets with $^1O_2^*$. The results indicate that the lability of membrane sites to photosensitization depends both on their inherent reactivity with $^1O_2^*$ and the relative location of specific protein and dye molecules.

Keywords: Photosensitization; Singlet oxygen; Plasma membrane; Photodynamic therapy; Membrane potential; Glucose transport; Proline transport; 5′-Nucleotidase

1. Introduction

Light-activated dyes have many uses in medicine and biology including photodestruction of tumor cells (photodynamic therapy) [1,2], deleting specific cell populations [3], causing focal thrombosis [4–6] and for treatments in dermatology [7]. The photochemical mechanism underlying these processes involves absorption of visible radiation by the dye molecules and subsequent formation of reactive intermediates such as singlet oxygen ($^1O_2^*$), superoxide anion ($O_2^{-\cdot}$) and dye radicals. These intermediates (or products formed from them) react rapidly with cellular proteins, lipids or nucleic acids. Typically, the desired effect is cytotoxicity although lower doses of dye and light cause more specific cellular effects.

Cell membranes are critical sites for photosensitized damage to cells. Little is known about which sites in membranes are most sensitive to photosensitized damage and how the sensitivity of sites varies with the location or distribution of the dye molecules in the membrane. This knowledge may lead to schemes for targeting of specific sites in membranes.

Many dye molecules partition into cellular membranes where, upon light activation, they may initiate photobiological responses. In some cases, the dyes distribute into all or most membranous structures and, in other cases, the photosensitizing dye may selectively localize in a specific membrane structure in cells such as the plasma membrane or inner mitochondrial membrane. Few previous studies have approached the differential sensitivity of membrane proteins to photosensitization. 5′-Nucleotidase was re-

Abbreviations: HBSS, Hank's balanced salt solution; HPS, Hepes physiological saline; MC540, merocyanine 540; RB, Rose bengal; $^1O_2^*$, singlet molecular oxygen; di-SBA-C_2(3) bis-oxonol, bis-(1,3-diethylthiobarbituric acid)trimethine oxonol; 3-MG, 3-*O*-methyl-D-glucose.

* Corresponding author. Fax: +1 (617) 7263192.

SSDI 0005-2736(94)00236-3

ported to be less labile to photosensitization than Na^+,K^+-ATPase using Photofrin as the photosensitizer [8] and photosensitized inhibition of amino acid transport was shown to occur at lower light doses than required for inhibition of facilitated glucose diffusion using hematoporphyrin derivative as the photosensitizer [9]. Another study suggested that a decrease in the membrane potential occurs at lower light doses than an increase in plasma membrane permeability [10].

In this study, two membrane photosensitizing dyes are used to investigate whether different functions of the plasma membrane (enzyme activity, transport of small molecules, maintenance of membrane potential, dye exclusion) have different sensitivities to light-initiated damage and, if so, what is the source of the differences. Possibilities include inherent lability of the different membrane components involved in each function, the location of the protein component in the plasma membrane, and the location of the photosensitizer in the membrane. Two dyes proposed for use in phototherapy, Rose bengal (RB) [5,6] and merocyanine 540 (MC540) [11], were chosen because they both localize in the plasma membrane of mammalian cells and are believed to cause cytotoxicity by generating $^1O_2^*$ which reacts with components of the plasma membrane [12,13]. A localized anionic group on both dye molecules inhibits deep penetration into, or through, the lipid bilayer. The geometry of MC540 in bilayers has been extensively studied because of its use as a membrane potential sensitive optical probe [14,15]. Because of the similarities between these two photosensitizers, the major variable between RB and MC540 for membrane photosensitization appeared to be their location in the membrane relative to the protein and lipid targets.

2. Materials and methods

2.1. Chemicals

The sources of the chemicals were as follows: Rose bengal and Trypan blue, Aldrich; merocyanine 540 and bis-(1,3-diethylthibarbituric acid)trimethine oxonol (di-SBA-C_2(3) bis-oxonol), Molecular Probes; 3-*O*-methyl-D-[^{3}H]glucose and L-[^{3}H]proline, [^{3}H]AMP, New England Nuclear or Amersham; phloretin, unlabelled 3-*O*-methyl-D-glucose, unlabelled L-proline, unlabelled AMP, sodium pyruvate, penicillin/streptomycin, magnesium chloride, α,β-methylene adenosine diphosphate, gramicidin and Hepes (*N*-2-hydroxyethylpiperazine-*N'*-2-ethane sulfonate), Sigma; RPMI-1740 media, L-glutamine, non-essential amino acids, fetal bovine serum, nystatin, and Hank's buffered salt solution (HBSS), Gibco Laboratories; scintillation cocktail (Liquiscint) National Diagnostics; oxygen (grade 4.4) and argon (grade 4.5) Airco Industrial Gases.

A RB stock solution at 0.265 mM was prepared in water using an absorption coefficient of $9.5 \cdot 10^4$ M^{-1} cm^{-1} at 548 nm [16]. This stock was diluted to give a final concentration of 4 μM RB for all experiments. A MC540 stock solution at 1.75 mM was prepared in water and used at 26 μM for all experiments. The concentrations of the dyes were chosen to be the highest which was non-toxic in the dark to the P388D_1 cells in order to minimize the irradiation times. Normalization for the number of photons of 514 nm radiation absorbed by dye molecules associated with cells was made as described below.

2.2. Cell culture

P388D_1 cells, a murine monocyte/macrophage cell line that grows in semi-suspension, were obtained from the Tumor Immunology Bank (ATCC). Cells were cultured in RPMI-1640 media containing 2 mM L-glutamine, 1 mM sodium pyruvate, 10 mM Hepes, 0.1 mM non-essential amino acids, 50 units/ml penicillin G, 0.05 mg/ml streptomycin, 50 units/ml nystatin, and 10% fetal bovine serum. Cells were cultured in 150 cm^2 Falcon brand flasks at 37°C with 5% CO_2 and harvested when confluent. The cells were released from the flask by gentle, sharp agitation, transferred to 50 ml centrifuge tubes and pelleted (5 min at approx. $150 \times g$). Cells were washed twice with HBSS before counting.

2.3. Absorption of 514 nm radiation by RB and MC540 associated with cells

P388D_1 cells ($20 \cdot 10^6$/ml) were incubated for 30 min with 4 μM RB or 26 μM MC540. The absorption spectrum of each suspension was measured from 400 to 700 nm using a suspension of cells at the same concentration without dye as the reference. The suspension was then centrifuged and the absorption spectra of the supernatant and that of the resuspended cells were recorded. The fraction of 514 nm radiation absorbed by dye associated with the cells was calculated from the difference in the absorbance at 514 nm of the original cell suspension minus that of the supernatant.

2.4. Uptake of RB and MC540 by cells

The uptake of RB by the cell suspension was calculated by comparing the absorption of the supernatant and the resuspended cells to a RB standard curve in PBS. Measurements were made at 563 nm, close to the absorption maximum of RB in membranes [17]. This method assumes that the extinction coefficient for RB in the cells and solution are the same. Our previous work showed about a 6% difference in the RB extinction coefficient between buffer and detergent [16]. For MC540 simple absorption measurements could not be used to determine uptake of dye by cells because the extinction coefficient of MC540

varied with environment and state of dye aggregation. After incubation ($15 \cdot 10^6$ cells/ml, 26 μM MC540), the fraction of MC540 in the cells was calculated by extracting the cell pellet with 0.1 ml 12 M HCl diluted to 2 ml with methanol. The absorption of this solution and the supernatant were measured separately at 555 and 528 nm, respectively. The amounts of dye present in the cells and the supernatant were determined by comparison with MC540 standards prepared in acidic methanol or HBSS for the cells and supernatant, respectively. Measurements were made with a Hewlett Packard 8451A diode array spectrophotometer.

2.5. Irradiations

The isolated 514 nm line from a cw argon ion laser (Innova 100, Coherent) was used. The beam was delivered via an optical fiber to a 0.5 cm^2 spot on the side of the sample cuvette, a 1 cm^2 quartz cuvette. The laser power was measured before and after irradiation using a calibrated power meter (model 210, Coherent). Typically, the laser power was 50 mW but was decreased or increased for experiments requiring lower or higher powers to deliver the radiation in 2–10 min.

Cell suspensions ($(20–30) \cdot 10^6$ cells/ml in 1 or 1.5 ml) were irradiated in 1 cm pathlength quartz septum-sealed cuvettes. The cells were maintained in suspension by gentle bubbling with oxygen. Cell suspensions were irradiated or maintained in the dark for an equal length of time as a control. All samples were transferred to 1.5 ml microcentrifuge tubes, wrapped in aluminum foil, and placed on ice until assays were performed (0.5–3 h). Cells were in HBSS until immediately before the assays.

2.6. Plasma membrane potential

The procedure of Specht and Rodgers [10] was followed with minor modifications. Briefly, after irradiation, cells ($20 \cdot 10^6$/ml) were immediately diluted with 6 ml ice-cold Hepes physiological saline (HPS) and placed on ice until measurements were made. The cells were then washed twice with cold HPS and resuspended at $(1–1.5) \cdot 10^6$ cells/ml. 3 ml of the cell suspension were added to a 1 cm quartz fluorescence cuvette and equilibrated at 37°C for 10 min; 1.5 μl of 1.5 mM di-SBA-C_2(3) bis-oxonol in DMSO was added and cells were equilibrated for 10 min longer. The fluorescence of samples was measured at 565 nm using excitation at 540 nm. Care was taken in establishing the excitation and emission wavelengths to minimize fluorescence of any RB and MC540 remaining in the cells after the washes. Complete depolarization was achieved by added 120 μl 1 M KCl and 10 μl gramicidin (0.2 mg/ml in DMSO). The fluorescence of the depolarized sample was measured after 10 min. The relative membrane potential was calculated as:

$$\text{Relative membrane potential} = \frac{F_0 - F_{exp}}{F_0 - F_f} \times 100$$

where F_0 = fluorescence of unirradiated control sample, F_{exp} = fluorescence of experimental sample, and F_f = fluorescence of completely depolarized sample. All measurements were made in triplicate. F_f values were at least 1.75-fold greater than F_0 values.

2.7. Glucose or proline uptake

Cell suspensions for proline uptake experiments were allowed to equilibrate for 30 min prior to the assay to ensure that inner amino acid pools were depleted before the assay. Isotope buffer (15 μl) for glucose uptake (60–100 μCi 3-*O*-methyl-D-[^{3}H]glucose (3-MG) plus 1 mM unlabelled 3-MG) or for proline uptake (100 μCi L-[^{3}H]proline plus 200 μM unlabelled L-proline) was placed in microcentrifuge tubes in a 37°C water bath. A 50 μl aliquot of irradiated or control cell suspension (also incubated at 37°C) was then discharged quickly from a micropipette onto the drops of buffer containing isotope with rapid mixing. At selected time intervals, the uptake was stopped with 1 ml of ice-cold stopping solution (300 μM phloretin plus 0.1 mM $HgCl_2$ in PBS for glucose uptake and PBS for proline transport). The suspensions were then centrifuged in a microfuge for 10 s. The supernatants were removed and the pellets were washed twice with ice-cold stopping solution. The samples were then transferred to scintillation vials, scintillation cocktail was added and the radioactivity of the samples was counted.

The rate of transport of proline into cells was determined by measuring the isotope in the cell pellet when the uptake was stopped 1.5, 3, 4.5, 6, and 7.5 min after mixing cells and buffer containing isotope-labeled proline. A blank sample to measure the amount of isotope non-specifically attached to the cells was prepared by quenching the uptake immediately after mixing. The average for this value in each experiment was subtracted from the value at each time point. All measurements were made in triplicate. Experiments using α-(methylamino)isobutyric acid, choline and 2-amino-2-norbornane carboxylic acid indicated that P388D_1 cells use the A transport system for amino acid uptake (data not shown) [18]. Control experiments showed that concentrations of 8 μM RB or 26 μM MC540 in the dark did not inhibit uptake of labeled proline by the cells.

The rate of facilitated glucose uptake was calculated from measurements similar to those for proline uptake except that the uptake of 3-MG was determined at 5, 10, 15, and 20 s after mixing cells and buffer containing labeled 3-MG. An equilibrium value for MG uptake was measured 10 min after mixing cells and isotope-containing buffer. A blank was measured as described above for glucose uptake and the average uptake by the blank was subtracted from the value for each time point. In each experiment, all measurements were made on triplicate aliquots of samples at each time point.

2.8. 5'-Nucleotidase activity

Samples (400 μl) to be assayed were diluted to final concentrations of 240 μM adenosine 5'-[^{3}H]monophosphate (AMP), 8.6 mM $MgCl_2$, 50 mM Tris (pH 6.9), and (3.6–5.3) · 10^6 cell/ml. The reactions were carried out at 37°C and the enzyme activity was terminated at 0, 3, 6, 9 and 12 min by transferring aliquots to 8 M formic acid on ice. Reaction products were separated by thin-layer chromatography on cellulose acetate sheets with fluorescent indicator (Eastman) in 30% methanol/water. The substrate, [^{3}H]AMP, was located by running nonradioactive AMP in comparison lanes. The lanes were cut into segments and the radioactivity was measured by liquid scintillation counting. The percent product at each time point was determined in triplicate. These kinetic data were used to determine the activity of 5'-nucleotidase. Percent inhibition was calculated from the slopes of the percent product versus time graphs for irradiated samples containing dye compared to non-irradiated samples containing dye.

2.9. Trypan blue exclusion

A 0.1 ml aliquot of the irradiated or control cell suspension was added to 2 ml of RPMI-1640 media and incubated at 37°C for varying periods of time (0.5, 6 or 24 h) in different experiments. A 1:1 mixture of cell suspension and 0.1% Trypan blue in PBS was used for counting total cells and cells taking up the dye using a hematocytometer. There was no difference in the results between counts made at 6 h and those at 24 h in the several experiments where this was tested.

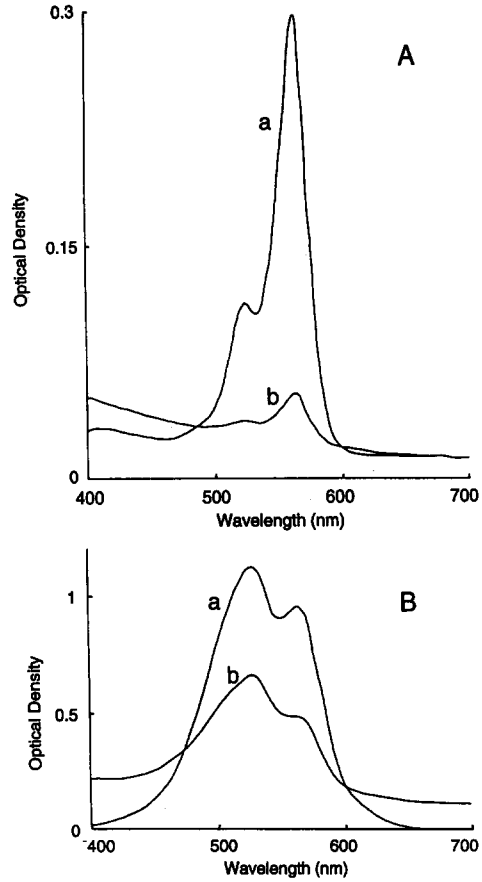

Fig. 1. Light absorption by Rose bengal and merocyanine 540 in cell suspensions. (A) Spectrum of 4 μM RB in P388D$_1$ cell suspensions (20 · 10^6 cells/ml) using a cuvette containing cells at the same concentration as the reference (curve a) or of supernatants after centrifugation of these suspensions using PBS as the reference (curve b). (B) Same types of spectra for 26 μM MC540 as shown for RB in (A). Absorption at 514 nm was determined as the difference between the total absorbance and the extrapolated baseline.

3. Results

3.1. Absorption of 514 nm radiation by RB and MC540 associated with cells

The fraction of incident radiation at 514 nm that is absorbed by molecules of RB and MC540 associated with cells must be known to calculate the relative effectiveness of the two photosensitizers per photon absorbed since dye molecules in solution do not contribute to the photosensitization process [19]. The absorption spectrum of 4 μM RB in a suspension of 20 · 10^6 cells/ml is shown in Fig. 1A using the cell suspension without RB as a reference. The absorption spectrum of the supernatant obtained after centrifuging the sample is also shown in Fig. 1A. The absorbances at 514 nm are 0.073 for RB plus cells and 0.007 for the supernatant (average of two experiments) indicating that the absorbance of RB in cells is 0.066 which corresponds to 14% absorption of the incident radiation.

The same types of absorption spectra measured for 26 μM MC540 are shown in Fig. 1B. The absorbance at 514 nm for MC540 in the cell suspension is 1.07 and that of the supernatant is 0.54. Subtracting these values yields an absorbance for MC540 in cells of 0.53 which corresponds to 70% absorption of the incident 514 nm radiation. Thus, at each incident dose in these experiments MC540 absorbs about 5-times as many photons at 514 nm than does RB. The values of 14% for RB and 70% for MC540 were used to convert incident light dose into absorbed light dose for all of the data shown. These absorption values are not corrected for scattering of the incident light by the cells which increases the pathlength. This effect does not influence comparisons between photosensitizers because the increase in absorption due to scattering will be the same for all samples.

3.2. Uptake of dyes by cells

Determination of RB uptake by cells with absorption measurements gave a value of 91% RB in cells. Extraction of MC540 from the cell pellet and supernatant gave a value of 67% MC540 associated with the cells based on

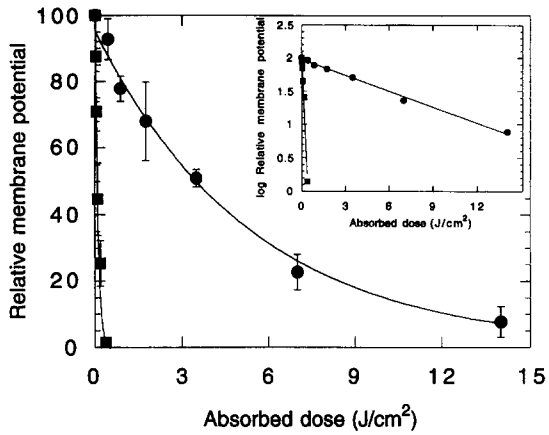

Fig. 2. Depolarization of the plasma membrane photosensitized by Rose bengal and merocyanine 540. Suspensions of P388D$_1$ cells were irradiated at 514 nm in the presence of either 4 μM RB (squares) or 26 μM merocyanine 540 (circles). The relative membrane potential was measured using di-SBA-C_2(3) bis-oxonol; control samples (dye, no light) were assigned a relative membrane potential value of 100. The absorbed dose of 514 nm radiation corresponds to the light absorbed only by dye molecules associated with the cells. The lines represent exponential fits of the data. The inset shows the data plotted according to first-order kinetics. The data are mean values for four experiments for RB and three experiments for MC540 and the error bars are standard deviations.

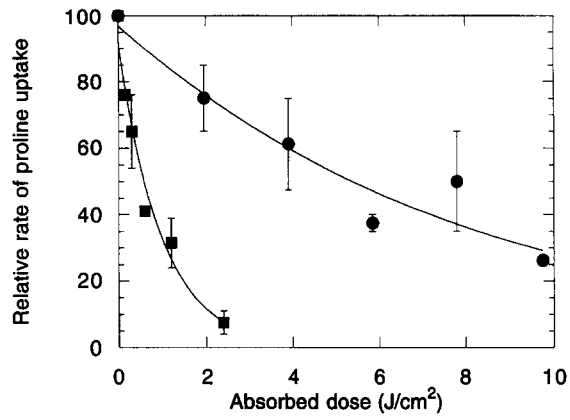

Fig. 3. Inhibition of proline uptake photosensitized by Rose bengal and merocyanine 540. Relative rates of L-[^{3}H]proline uptake by P388D$_1$ cells in the presence of either 4 μM RB (squares) or 26 μM MC540 (circles) are plotted versus absorbed dose of 514 nm light. Control samples (dye, no light) were assigned a relative value of 100. The absorbed dose of 514 nm radiation corresponds to the light absorbed only by dye molecules associated with the cells. The lines represent exponential fits of the data. The standard deviation of triplicate measurements at each time point in a kinetic experiment was typically 10–15% of the value. The data shown are the mean values from the two experiments; the error bars are the range of values obtained.

93% recovery of the dye (average of two experiments).

3.3. Photosensitized depolarization of plasma membrane

Plasma membrane potential was monitored using the dye di-SBA-C2(3) bis-oxonol. Neither RB nor MC540 caused a membrane potential change in the dark, and 20 J/cm^2, the highest incident dose, did not affect the membrane potential in the absence of photosensitizing dyes. The polarization was measured relative to unirradiated, dye-treated cells; KCl and gramicidin were used to completely depolarize cells and establish the background fluorescence. The data from four experiments using RB and three experiments using MC540 are shown in Fig. 2.

In order to compare quantitatively the photosensitization efficiency of the two dyes for the five types of membrane function, the energy absorbed by the dye associated with the cells which causes a 50% change for each membrane function was calculated. This value was called the P_{50}. The P_{50} was calculated from the slopes of plots of log (membrane function) vs. absorbed dose such as those shown in the inset of Fig. 2. The linearity of these plots (correlation coefficient > 0.98) indicates that the photosensitization process follows first order kinetics. The P_{50} values obtained showed that RB is about 46-times more effective than MC540 at photosensitizing the depolarization of the plasma membrane (Table 1).

3.4. Photosensitized inhibition of proline transport

The time-dependent uptake of L-[^{3}H]proline was used to monitor the effect of photosensitization on the proline transporter. Uptake by the cells was linear with time up to at least 8 min after mixing of cells and labeled L-[^{3}H]proline (data not shown). Irradiation at 514 nm of samples containing 4 μM RB and (20–30) · 10^6 cells/ml produced a dose-dependent decrease in the rate of labeled proline uptake by the cells. The average slopes of the uptake

Table 1
Photosensitized change in plasma membrane functions of P388D$_1$ cells using Rose bengal and merocyanine 540 with 514 nm irradiation

Membrane function	Dose absorbed to produce 50% change (P_{50}, J/cm^2) [a]		
	Rose bengal	merocyanine 540	ratio
Membrane potential	0.08 ± 0.01	3.5 ± 0.4	46 ± 11
Proline uptake	0.58 ± 0.06	5.4 ± 0.8	9.2 ± 2.4
Glucose transport	3.1 ± 0.4	7.0 ± 1.1	2.3 ± 0.7
5′-Nucleotidase	15 ± 2 [b]	85 ± 33 [b]	5.7 ± 2.4
Membrane permeability	3.4 ± 0.8	35 ± 9	10 ± 3.1

[a] Mean value and standard deviation.
[b] Extrapolated value; see text.

curves from two independent experiments are plotted versus absorbed dose in Fig. 3. The data have been normalized to a value of 100 for unirradiated, RB-containing samples since the absolute value for the rate of proline uptake varied from day-to-day. The data for all of the other measurements described below have been normalized in the same way. Experiments with MC540 were performed using 26 μM dye and the same cell concentration. Similar dose-dependent decreases in the rates of proline uptake were observed (Fig. 2) but MC540 was markedly less efficient than RB as a photosensitizer. The slopes of plots of log (rate of proline uptake) versus absorbed dose gave P_{50} values showing that RB is about 9-times more efficient than MC540 (Table 1); correlation coefficients for the slopes were > 0.96.

3.5. Photosensitized inhibition of facilitated glucose diffusion

The uptake of 3-[^{3}H]MG, a non-metabolized glucose analog, was measured at 5, 10. 15, and 20 s after mixing with the cells. The uptake was linear with time until about at least 30 s (data not shown). After 20 s the uptake of labeled 3-MG by untreated samples was typically 0.8% of the total isotope in the solution. The linearity of the uptake versus time plots indicates that diffusion out of the cells was not significant during the measurement period. In the dark, neither RB nor MC540 inhibited glucose diffusion at the concentrations used.

Irradiation at 514 nm of cell suspensions containing 4 μM RB or 26 μM MC540 decreased the rate of 3-MG uptake in a dose dependent manner. The relative rates of glucose diffusion into cells are shown as a function of absorbed 514 nm energy in Fig. 4. The P_{50} values calculated as described above indicate that RB is about 3-times more efficient than MC540 for photosensitizing inhibition of glucose transport; correlation coefficients for the slopes of the semi-log plots were > 0.97.

3.6. Photosensitized inhibition of 5′-nucleotidase activity

5′-Nucleotidase activity was measured by the rate of cleavage of [^{3}H]AMP. 5′-Nucleotidase activity in the P388D$_1$ cells was shown to be inhibited by α,β-methylene adenosine diphosphate indicating that the ectoenzyme activity was being measured (data not shown). This membrane activity was much more resistant to photosensitization than any of the others measured. Even at the highest absorbed dose (15 J/cm^2 for RB and 35 J/cm^2 for MC540), the extent of photosensitized inhibition was limited to about 30% (Fig. 5). These high light doses caused significant bleaching of the photosensitizers which contributed to the low apparent efficiency of photosensitization of 5′-nucleotidase. This is also apparent from the relatively poor exponential fit of the data in Fig. 5. At the lower light doses used in other experiments, photobleaching was not important since the log (membrane function) vs. absorbed dose plots were linear. Because of photobleaching, only the initial slopes were used to estimate the relative efficiencies of RB and MC540 for photosensitization of 5′-nucleotidase. P_{50} values for RB and MC540 were estimated to be at least 85 and 15 J/cm^2, respectively; correlation coefficients for the slopes of semi-log plots were > 0.94.

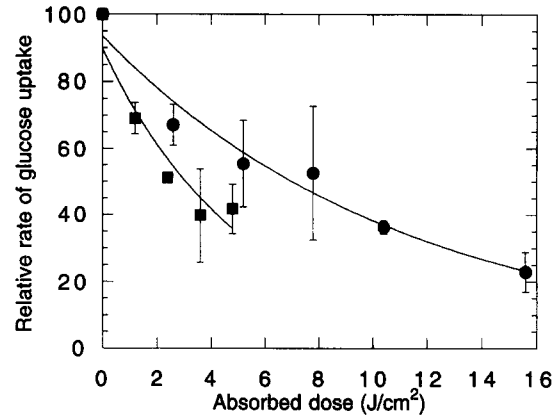

Fig. 4. Inhibition of facilitated glucose transport photosensitized by Rose bengal and merocyanine 540. Relative rates of uptake of 3-*O*-methyl-D-[^{3}H]glucose by P388D$_1$ cells in the presence of either 4 μM RB (squares) or 26 μM MC540 (circles) are plotted versus absorbed dose of 514 nm light. Control samples (dye, no light) were assigned a relative value of 100. The absorbed dose of 514 nm radiation corresponds to the light absorbed only by dye molecules associated with the cells. The lines represent exponential fits of the data. The data are from a typical experiment for each dye and the error bars are the standard deviations of triplicate measurements.

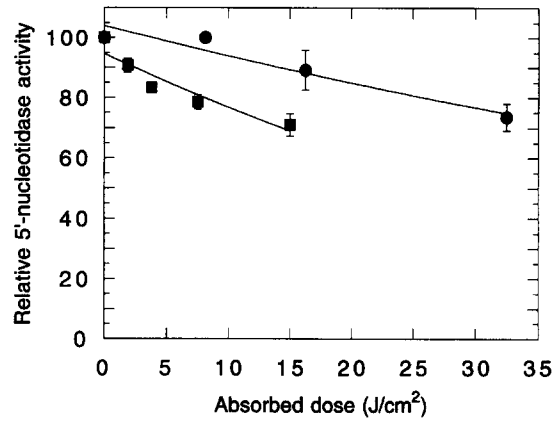

Fig. 5. Inhibition of 5′-nucleotidase activity photosensitized by Rose bengal and merocyanine 540. The rates of conversion of [^{3}H]AMP to [^{3}H]adenosine by P388D$_1$ cells in the presence of either 4 μM RB (squares) or 26 μM MC540 (circles) are plotted versus absorbed dose of 514 nm light. Control samples (dye, no light) were assigned a relative value of 100. The absorbed dose of 514 nm radiation corresponds to the light absorbed only by dye molecules associated with the cells. The lines represent exponential fits of the data. The data shown have been combined from three experiments for RB and two experiments for MC540. The error bars are standard deviations.

3.7. Photosensitized change in dye exclusion

The percent of P388D$_1$ cells that were stained by Trypan blue was measured in some of the experiments described above for photosensitized inhibition of the other membrane functions. Prior to light treatments the values for percent of Trypan blue permeable cells was typically < 5% but occasionally up to 20%. The light doses delivered were, in most cases, not sufficiently high to cause uptake of Trypan blue by 50% of the cells. Considerable variability was found in the results obtained when the assay was performed in conjunction with different experiments. The exclusion of Trypan blue has been reported to be subject to many factors [20]. A P_{50} value of 3.4 J/cm^2 for membrane permeability was estimated from experiments measuring RB-photosensitized inhibition of 5′-nucleotidase activity. In the same experiments, a P_{50} value of 35 J/cm^2 was extrapolated from the data for MC540 photosensitization. In experiments measuring glucose uptake, the highest absorbed light doses (4.8 J/cm^2 for RB, 17 J/cm^2 for MC540) caused less than 50% uptake of Trypan blue. A similar result was obtained for measurements made as part of the experiments on inhibition of proline uptake where even lower absorbed doses were used. Thus, the P_{50} values in Table 1 are those obtained from the 5′-nucleotidase experiments but are consistent with the results from the other experiments. This result indicates that all of the membrane functions except 5′-nucleotidase activity were more sensitive to photosensitization than membrane permeability to Trypan blue.

4. Discussion

The results of this study demonstrate that a simple model for membrane photosensitization in which dye molecules are homogeneously distributed and all sites are equally sensitive to light-induced inhibition cannot be used even for two dyes that localize in the plasma membrane and generate $^1O_2^*$ upon light activation. As shown in Table 1, the five plasma membrane functions vary over a wide range in their sensitivity to photosensitized inhibition or alteration using RB or MC540 as the photosensitizer; the range of P_{50} values for RB is 188 but the range for MC540 is only about 24. In addition, the relative ordering of sensitivities to photosensitization by RB or MC540 differs markedly. The P_{50} values are lower than those for MC540 although by varying amounts for the different membrane functions studied.

Two distinct models for membrane photosensitization by dyes can be considered to gain perspective on the photosensitization process. In the simplest model, the photosensitizing dye molecules are evenly distributed throughout the entire area of the membrane and do not bind to specific proteins. The relative sensitivities of membrane proteins or lipids to photosensitization, according to this model, is directly related to their inherent reactivity with the toxic species produced upon photoexcitation of the dyes and their location (integral membrane protein versus surface bound). This model predicts that for any site of damage, the ratio of P_{50} values for RB and MC540 will be constant. Support for this model is available from studies of eosin placed at two different locations in red cell membranes; photosensitization of red cell lysis and of acetylcholinesterase inhibition was independent of dye location [21]. The simple model is consistent with a picture of dye photosensitization occurring by a common mechanism for all photosensitizers; increasing photosensitization efficiency occurs by increasing the yield of toxic species formed by photoexcitation of the dye and targeting of specific membrane proteins is not possible.

The other distinct model, 'specific' photosensitization, involves binding of dye molecules to specific sites (most probably membrane proteins) with different binding constants; the photosensitization efficiency is assumed to be regulated mainly by the proximity of the dye and protein. Each dye would have a unique set of binding constants with membrane proteins. This model predicts that a wide range of P_{50} values will be found for any single photosensitizer. A variation in the ratio of P_{50} values for any pair of photosensitizing dyes is expected. This model also suggests that specific proteins, those with the highest sensitivity to photosensitization (low P_{50} value) could be selectively 'targeted' with the proper photosensitizing dye.

4.1. Photosensitization by RB

The P_{50} values for RB cover a 188-fold range indicating that RB photosensitizes mainly by a 'specific' mechanism. The membrane potential was the most efficiently photosensitized membrane function. The high selectivity for this function by RB photosensitization can be attributed to binding of RB to proteins regulating the plasma membrane potential such as the K^+ leak channel and Na^+,K^+-ATPase. The membrane potential for cells such as the P388D$_1$ cells (a monocyte/macrophage line) is expected to be due to K^+ selective membrane permeability and is generally maintained by the K^+ leak channel and plasma membrane Na^+,K^+-ATPase, both integral membrane protein. When RB is bound to a protein, the $^1O_2^*$ molecules react with the protein without diffusing through the membrane which contains reactive unsaturated lipid and protein amino acids. Alternatively, binding of RB to a membrane target may facilitate a non-$^1O_2^*$ mechanism between an excited state of RB and the target. The high sensitivity of the membrane potential to RB photosensitization may be useful since many cell functions are altered by depolarization of the plasma membrane and photosensitization by RB may be a way to alter the membrane potential while having little effect on other membrane proteins.

The P_{50} values for proline transport and facilitated glucose diffusion which involve integral membrane pro-

teins vary by a factor of four. These integral membrane proteins appear to have similar reactivity with $^1O_2^*$ (based on similar P_{50} values with MC540, see below) suggesting that RB shows a low degree of selective binding to these proteins. The photosensitization may be initiated partially through light absorption by RB molecules that are not bound to the target, i.e., by the 'simple' mechanism.

The low sensitivity of 5′-nucleotidase for RB photosensitization (high P_{50} value) is consistent with its location on the outer surface of the membrane where it is anchored in the lipid bilayer by a glycosyl phosphatidylinositol group [22]. 5′-Nucleotidase has previously been shown to be less sensitive than Na^+,K^+-ATPase to photosensitization using Photofrin as the dye [8]. The significantly higher P_{50} value for 5′-nucleotidase compared to the transmembrane proteins can be attributed to the requirement that $^1O_2^*$ molecules escape the membrane location where they are formed in order to reach this enzyme.

4.2. Photosensitization by MC540

Consideration of the data for MC540 in Table 1 suggests that this dye may be relatively evenly distributed over the area of the plasma membrane. Three of the plasma membrane functions (proline uptake, glucose transport, and membrane potential) had low P_{50} values that only vary by a factor of two (3.5 and 7.0 J/cm^2). This result would be expected if MC540 were uniformly distributed across the area of the plasma membrane and if the proteins involved in these functions had approximately the same inherent sensitivity to inhibition by reaction with $^1O_2^*$. The small differences in the lability of these targets to photosensitization can be attributed to either variation in localization of MC540 or inherent reactivity of the target with $^1O_2^*$. The proline and glucose transporters, Na^+,K^+-ATPase and K^+ leak channel are integral membrane proteins with one or more transmembrane domains. Since all of these proteins involve transport of molecules or ions across the membrane, the transmembrane portion is essential for their proper action. Assuming that the transmembrane regions of these proteins do not contain unusual amino acid composition, similar P_{50} values are expected.

Assuming that the inherent reactivity of 5′-nucleotidase is the same as those of the transmembrane proteins studied, the difference in P_{50} values indicates that $^1O_2^*$ molecules generated from photoexcitation of MC540 have about 12–24 fold greater probability of diffusing through the membrane and reacting with the proteins than of diffusing out of the membrane and reacting with proteins extending from the surface of the membrane.

The P_{50} value for photosensitization of membrane permeability to Trypan blue, is significantly higher than those for the transmembrane proteins suggesting that a significant amount of chemical damage must occur to membrane components to produce a measurable change in permeability to this dye. The specific damage to membranes that causes an increase in the membrane permeability to Trypan blue may involve both protein and membrane sites.

4.3. Singlet oxygen yields of RB and MC540 in plasma membranes

If RB and MC540 both photosensitized by the simple mechanism described above, the ratio of P_{50} values for inhibition of each membrane function should be constant and reflect the relative $^1O_2^*$ yields produced per photon absorbed by each dye (assuming that the phototoxicity mechanism is dominated by $^1O_2^*$ as the toxic species). This value can be estimated to be about 150 if the quantum yield for $^1O_2^*$ is 0.75 for RB in membranes [23,24] and 0.005 for MC540. The latter value was estimated from the quantum yield for MC540 triplets in phosphatidylcholine liposomes (0.01–0.09 given by Aramendia et al. [25]), assumes 100% efficiency for transfer of energy from triplet MC540 to O_2, and an estimate that 10% of the MC540 molecules associated with cell membranes under our conditions are monomers as determined from the absorption spectra (Fig. 1B). This value is consistent with that measured by oxygen consumption for MC540 in erythrocyte membranes [26]. Only the absorption of monomers is considered because photosensitization by the monomer dominates over that by the dimers [26]. The ratio of P_{50} values shown in Table 1 are all significantly below 150 indicating that RB is less efficient or MC540 is more efficient as a photosensitizer than predicted from their $^1O_2^*$ quantum yields. The reason for this divergence cannot be determined from our data but possibilities include: an efficient non-$^1O_2^*$ mechanism for photosensitization by MC540 in membranes (such as toxic photoproduct formation [27]), quenching of RB triplet in membranes, and localization of RB closer to the extracellular surface of the membrane than MC540 so that more of the $^1O_2^*$ diffuses from the membrane and is unavailable for reacting with membrane components.

The establishment that the photosensitization mechanism for some photosensitizers involves specific interaction of the dye with membrane proteins adds additional complexity to modeling of the photosensitization process. These models have assumed relatively even distribution of photosensitizers in the membrane to calculate $^1O_2^*$ lifetimes and the fraction of $^1O_2^*$ molecules that diffuse from the membrane [28].

4.4. Conclusions

Generalization of these results indicates that the photosensitizing efficiency of other dyes in membranes may not correlate with their $^1O_2^*$ yields in solution because of specific associations in the membranes. In fact, the variation in P_{50} ratio shown in Table 1 suggests that predictions cannot even be made between two photosensitizers and their effects on a series of membrane functions. At-

tempts to improve photosensitization efficiency or to use photosensitization to target specific membrane proteins or functions requires further knowledge of the specific membrane photosensitization mechanisms.

Acknowledgements

Support of this research NIH grant R01 GM30755 is gratefully acknowledged.

References

[1] Henderson, B.W. and Dougherty, T.J. (1992) Photochem. Photobiol. 55, 145–157.
[2] Moan, J. and Berg, K. (1992) Photochem. Photobiol. 55, 931–948.
[3] Madison, R., Macklis, J.D. and Thies, C. (1990) Brain Res. 522, 90–98.
[4] Dietrich, W.D., Watson, B.D., Busto, R., Ginsberg, M.D. and Bethea, J.R. (1987) Acta Neuropathol. (Berl) 72, 315–325.
[5] Dietrich, W.D., Prado, R. and Watson, B.D. (1988) Stroke 19, 857–862.
[6] Huang, A.J.W., Watson, B.D., Hernandez, E. and Tseng, S.C.G. (1988) Arch. Ophthalmol. 106, 680–685.
[7] Lui, H. and Anderson, R.R. (1992) Arch. Derm. 128, 1631–1636.
[8] Gibson, S.L., Murant, R.S. and Hilf, R. (1988) Cancer Res. 48, 3360–3366.
[9] Dubbelman, T.M.A.R. and Van Steveninck, J. (1984) Biochim. Biophys. Acta 771, 201–207.
[10] Specht, K.G. and Rodgers, M.A.J. (1990) Photochem. Photobiol. 51, 319–324.
[11] Sieber, F. (1987) Photochem. Photobiol. 46, 1035–1042.
[12] Kalyanaraman, B., Feix, J.B., Sieber, F., Thomas, J.P. and Girotti, A.W. (1987) Proc. Natl. Acad. Sci. USA 84, 2999–3003.
[13] Valenzeno, D.P., Trudgen, J., Hutzenbuhler, A. and Milne, M. (1987) Photochem. Photobiol. 46, 985–990.
[14] Dragsten, P.R. and Webb, W.W. (1978) Biochem. 17, 5228–5240.
[15] Verkman, A.S. (1987) Biochem. 26, 4050–4056.
[16] Allen, M.T., Lynch, M., Lagos, A., Redmond, R.W. and Kochevar, I.E. (1991) Biochim. Biophys. Acta 1075, 42–49.
[17] Fluhler, E.N., Hurley, J.K. and Kochevar, I.E. (1990) Biochim. Biophys. Acta 990, 269–275.
[18] Christensen, H.N. (1989) Methods Enzymol. 173, 576–616.
[19] Valenzeno, D.P. and Pooler, J.P. (1982) Photochem. Photobiol. 35, 343–350.
[20] Krause, A.W., Carley, W.W. and Webb, W.W. (1984) J. Histochem. Cytochem. 32, 1084–1090.
[21] Pooler, J.P. (1989) Photochem. Photobiol. 50, 55–68.
[22] Zimmermann, H. (1992) Biochem. J. 285, 345–365.
[23] Murasecco-Suardi, P., Gassmann, E., Braun, A.M. and Oliveros, E. (1987) Helv. Chim. Acta 70, 1760–1773.
[24] Lee, P.C.C. and Rodger, M.A.J. (1987) Photochem. Photobiol. 45, 79–86.
[25] Aramendia, P.F., Krieg, M., Nitsch, C., Bittersmann, E. and Braslavsky, S.E. (1988) Photochem. Photobiol. 48, 187–194.
[26] Singh, R.J., Feix, J.B., Pintar, T.J., Girotti, A.W. and Kalyanaraman, B. (1991) Photochem. Photobiol. 53, 493–500.
[27] Davila, J., Harriman, A. and Gulliya, K.S. (1991) Photochem. Photobiol. 53, 1–11.
[28] Kanofsky, J.R. and Baker, A. (1993) Photochem. Photobiol. 57, 720–727.